J|A|C|S
ARTICLES
Published on Web 08/23/2003

Novel Route to Periodic Mesoporous Aminosilicas, PMAs: Ammonolysis of Periodic Mesoporous Organosilicas

Tewodros Asefa,[†] Michal Kruk,[‡] Neil Coombs,[†] Hiltrud Grondey,[†] Mark J. MacLachlan,[†] Mietek Jaroniec,[‡] and Geoffrey A. Ozin*,[†]

Contribution from the Materials Chemistry Research Group, Department of Chemistry, University of Toronto, 80 St. George Street, Toronto, Ontario, M5S 3H6, Canada, and Department of Chemistry, Kent State University, Kent, Ohio 44240

Received May 12, 2003; E-mail: gozin@alchemy.chem.utoronto.ca

Abstract: A new route to periodic mesoporous aminosilicas (PMAs) that contain amine functional groups in the framework of a mesoporous network is reported. The materials are prepared via thermal ammonolysis of periodic mesoporous organosilicas (PMOs) under a flow of ammonia gas. PMOs integrate similar or even higher quantities of nitrogen-containing groups upon ammonolysis than similarly treated ordered mesoporous silicas (MCM-41). The quantity of amine groups introduced into the materials was found to depend strongly on the ammonolysis temperature. The largest loading of amine groups was obtained when a well-ordered cubic methylene PMO material without prior vacuum-drying was thermolyzed in ammonia. The ordered mesoporosity of PMOs was preserved during the ammonolysis with only a slight decrease in the mesopore size and the degree of mesostructural ordering. The extent of substitution of framework oxygen by amine and nitride groups was established by solid-state ^{29}Si CP-MAS, ^{29}Si MAS, ^{15}N MAS, and ^{13}C CP-MAS NMR spectroscopies, elemental analysis, and X-ray photoelectron spectroscopy. In some cases, methylene and methyl functional groups were also present in the PMAs along with amine functional groups, as inferred from elemental analysis and gas adsorption, particularly in cases where PMOs were subjected to ammonolysis at 400 and 550 °C for several hours. This resulted in new multifunctional mesoporous organoaminosilica nanomaterials with properties that could be tuned by systematically varying the relative amounts of hydrophilic amine and hydrophobic hydrocarbon pendent and framework groups. The stability upon storage was found to be much higher for PMAs obtained from PMOs than for those obtained from MCM-41 silicas under the same conditions.

Introduction

Since the first publications on surfactant-templated mesoporous materials appeared about 10 years ago,[1] a vast number of materials with mesoporous structures having various compositions have been synthesized.[2,3] Furthermore, many potential applications that exploit the high surface area, uniform pore size, well-defined pore shape and periodic structure of these materials have been demonstrated in catalysis, adsorption, separation, sensing and nanotechnology.[4] Many of these materials have inorganic frameworks and are commonly synthesized through a combination of sol−gel and self-assembly techniques from a mixture of metal alkoxides and organic supramolecular templates in the presence of acid or base catalysts. The removal of the organic templates from the resulting materials creates ordered mesoporous structures that have high surface areas and pore volumes. Recently, the introduction of organic functional groups into these periodic mesoporous silicas, which are the most prominent group of surfactant-templated mesoporous materials, has become increasingly important, primarily due to the fact that the silica framework does not contain active functional sites

[†] Materials Chemistry Research Group, Department of Chemistry, University of Toronto.

[‡] Department of Chemistry, Kent State University.

(1) (a) Kresge, C. T.; Leonowicz, M. E.; Roth, W. J.; Vartuli, J. C.; Beck, J. S. *Nature* **1992**, *359*, 710−712. (b) Beck, J. S.; Vartuli, J. C.; Roth, W. J.; Leonowicz, M. E.; Kresge, C. T.; Schmitt, K. D.; Chu, C. T.-W.; Olson, D. H.; Sheppard, E. W.; McCullen, S. B.; Higgins, J. B.; Schlenker, J. L. *J. Am. Chem. Soc.* **1992**, *114*, 10 834−10 843. (c) Yanagisawa, T.; Shimizu, T.; Kuroda, K.; Kato, C. *Bull. Chem. Soc. Jpn.* **1990**, *63*, 988−992. (d) Inagaki, S.; Fukushima, Y.; Kuroda, K. *J. Chem. Soc., Chem. Commun.* **1993**, 680−682.

(2) (a) Antonelli, D. M.; Ying, J. Y. *Angew. Chem., Int. Ed. Engl*. **1996**, *35*, 426−430. (b) Tian, Z.-R.; Tong, W.; Wang, J.-Y.; Duan, N.-G.; Krishnan, V. V.; Suib, S. L. *Science* **1997**, *276*, 926−930.

(3) (a) Braun, P. V.; Osenar, P.; Stupp, S. I. *Nature* **1996**, *380*, 325−328. (b) MacLachlan, M. J.; Coombs, N.; Ozin, G. A. *Nature* **1999**, *397*, 681−684. (c) Rangan, K. K.; Billinge, S. J. L.; Petkov, V.; Heising, J.; Kanatzidis, M. G. *Chem. Mater.* **1999**, *11*, 2629−2632. (d) MacLachlan, M. J.; Coombs, N.; Bedard, R. L.; White, S.; Thompson, L. K.; Ozin, G. A. *J. Am. Chem. Soc.* **1999**, *121*, 12 005−12 017. (e) Attard, G. S.; Göltner, C. G.; Corker, J. M.; Henke, S.; Templer, R. H. *Angew. Chem., Int. Ed. Engl.* **1997**, *36*, 1315−1317. (f) Yang, P.; Zhao, D.; Margolese, D. I.; Chmelka, B. F.; Stucky, G. D. *Nature* **1998**, *396*, 152−155.

(4) (a) Sayari, A. *Chem. Mater.* **1996**, *8*, 1840−1852. (b) Corma, A. *Chem. Rev.* **1997**, *97*, 2373−2419. (c) Moller, K.; Bein, T. *Chem. Mater.* **1998**, *10*, 2950−2963. (d) Vartulli, J. C.; Shih, S. S.; Kresge, C. T.; Beck, J. S. *Stud. Surf. Sci. Catal.* **1998**, *117*, 13−21. (e) Ying, J. Y.; Mehnert, C. P.; Wong, M. S. *Angew. Chem., Int. Ed. Engl.* **1999**, *38*, 56−77. (f) Stein, A.; Melde, B. J.; Schroden, R. C. *Adv. Mater.* **2000**, *12*, 1403−1419. (g) Tajima, K.; Aida, T. *Chem. Commun.* **2000**, 2399−2412. (h) Wirsberger, G.; Stucky, G. D. *ChemPhysChem* **2000**, *1*, 89−92. (i) Sayari, A.; Hamoudi, S. *Chem. Mater.* **2001**, *13*, 3151−3168. (j) Schuth, F. *Chem. Mater.* **2001**, *13*, 3184−3195. (k) Trong On, D.; Desplantier-Giscard, D.; Kaliaguine, S. *Appl. Catal. A: General* **2001**, *222*, 299−357. (l) Davis, M. E. *Nature* **2002**, *417*, 813−821. (m) De Vos, D. E.; Dams, M.; Sels, B. F.; Jacobs, P. A. *Chem. Rev.* **2002**, *102*, 3615−3640. (n) Schuth, F.; Schmidt, W. *Adv. Mater.* **2002**, *14*, 629−638.

10.1021/ja036080z CCC: $25.00

that are essential for many applications. In earlier studies, organic groups have been incorporated into ordered mesoporous silicas through direct co-assembly or post-synthesis grafting of organotrialkoxysilanes $RSi(OR')_3$ resulting in terminally bonded organic groups housed inside the pores.[1b,5] More recently, it was shown to be possible to introduce organic groups within the inorganic framework itself by using precursors with organic groups bonded to two or more trialkoxysilyl groups.[6] This synthetic approach afforded a novel class of ordered mesoporous materials, periodic mesoporous organosilicas (PMOs), with hybrid organic−inorganic frameworks that can have controlled loadings of bridging organic groups, and a range of new chemical, physical and surface properties.[6]

The synthesis of PMOs has led to the introduction of alkane, alkene, aromatic, and organometallic functional groups into the channel walls.[6] However, there have been only a few attempts to introduce nitrogen-containing groups in PMOs. These include the synthesis of a pyridine-bridged PMO, which did not have a well-defined structure or good stability,[7a] and the syntheses of ordered materials with a fraction of nitrogen-containing bis(trialkoxysilyl)organic groups supposedly incorporated in the silica frameworks.[7b−d] In the latter cases,[7b−d] the bridging organic groups include flexible chain fragments that likely lead to mechanically unstable organosilicate frameworks.[7a,8] Moreover, these bridging groups were probably too large to be intimately mixed with the silica framework. These considerations suggest that the aforementioned nitrogen-containing bridging organic groups might be located on the pore surface instead of in the framework,[7b−d] similar to the well-known and extensively studied mesoporous silicas with terminal (surface-bonded) organomonoamine and organopolyamine functional groups.[9−11] These nitrogen-containing functional groups, namely amine, diamine, and triamine groups,[9] and cyclams,[11a] can allow such materials to be used as solid base catalysts or to function as ligands to anchor metal ions or organometallic groups for metal based catalysis and other applications.[9−13] Furthermore, the amine groups could be reactive and hydrophilic enough to allow immobilization of analytes and to scavenge toxic anions and heavy metals from waste streams.[9c,10b]

Other nitrogen and amine containing materials such as silicon oxynitrides (SONs) and nitrogen containing silicate glasses have been synthesized by high-temperature treatment of silicon dioxide powders and thin films in ammonia.[14,15] The thermally induced substitution of two-coordinate oxygen by three-coordinate nitrogen in a silica network is known to confer many unique properties to the SON materials such as high dielectric constant, dielectric breakdown strength and resistance to oxidation.[14g] These properties in turn make these materials potentially useful as impurity diffusion masks and substrates for microelectronic device applications.[14i]

The hydrolytic instability of Si−N bonds hinders the synthesis of amine-functionalized silica materials from aminoalkoxysilane precursors in aqueous conditions at lower temperatures through the traditional sol−gel route. In this regard, the first successful chemical route to aminosilica materials containing Si−N bonds was reported by Bradley and co-workers.[16] They used a nonaqueous ammonolytic sol−gel method to make amorphous silicon diimide gels. Later, further progress has been made in the synthesis of disordered microporous and mesoporous silicon oxynitrides in nonaqueous media.[17] The formation of pores in some of these materials was suggested to involve the templating by salt nanocrystals.[17a] In another case, the pore sizes reflected the dimensions of single porogen molecules.[17c] However, the thermally driven ammonolysis still remains the most promising method to introduce nitrogen directly into silica-based ordered porous materials.[15]

(5) (a) Yanagisawa, T.; Shimizu, T.; Kuroda, K.; Kato, C. *Bull. Chem. Soc. Jpn.* **1990**, *63*, 1535−1537. (b) Burkett, S. L.; Sims, S. D.; Mann, S. *Chem. Commun.* **1996**, 1367−1368. (c) Macquarrie, D. J. *Chem. Comm.* **1996**, 1961−1962. (d) Mori, Y.; Pinnavaia, T. J. *Chem. Mater.* **2001**, *13*, 2173−2178. (e) Kruk, M.; Asefa, T.; Jaroniec, M.; Ozin, G. A. *J. Am. Chem. Soc.* **2002**, *124*, 6383−6392.

(6) (a) Asefa, T.; MacLachlan, M. J.; Coombs, N.; Ozin, G. A. *Nature* **1999**, *402*, 867−871. (b) Inagaki, S.; Guan, S.; Fukushima, Y.; Ohsuna, T.; Terasaki, O. *J. Am. Chem. Soc.* **1999**, *121*, 9611−9614. (c) Melde, B. J.; Holland, B. T.; Blanford, C. F.; Stein, A. *Chem. Mater.* **1999**, *11*, 3302−3308. (d) Yoshina-Ishii, C.; Asefa, T.; Coombs, N.; MacLachlan, M. J.; Ozin, G. A. *Chem. Commun.* **1999**, 2539−2540. (e) Asefa, T.; MacLachlan, M. J.; Grondey, H.; Coombs, N.; Ozin, G. A. *Angew. Chem., Int. Ed. Engl.* **2000**, *39*, 1808−1811. (f) Sayari, A.; Hamoudi, S.; Yang, Y.; Moudrakovski, I. L.; Ripmeester, J. R. *Chem. Mater.* **2000**, *12*, 3857−3863. (g) Dag, Ö.; Yoshina-Ishii, C.; Asefa, T.; MacLachlan, M. J.; Grondey, H.; Ozin, G. A.; *Adv. Funct. Mater.* **2001**, *3*, 213−217. (h) Lu, Y.; Fan, H.; Doke, N.; Loy, D. A.; Assink, R. A.; LaVan, D. A.; Brinker, C. J. *J. Am. Chem. Soc.* **2000**, *122*, 5258−5261. (i) Asefa, T.; Kruk, M.; MacLachlan, M. J.; Coombs, N.; Grondey, H.; Jaroniec, M.; Ozin, G. A. *J. Am. Chem. Soc.* **2001**, *35*, 8520−8530. (j) Burleigh, M. C.; Dai, S.; Hagaman, E. W. *Chem. Mater.* **2001**, *13*, 2537−2546. (k) Temtsin, G.; Asefa, T.; Bittner, S.; Ozin, G. A. *J. Mater. Chem.* **2001**, *11*, 3202−3206. (l) Inagaki, S.; Guan, S.; Ohsuna, T.; Terasaki, O. *Nature* **2002**, *416*, 304−307. (m) Kapoor, M. P.; Yang, Q.; Inagaki, S. *J. Am. Chem. Soc.* **2002**, *124*, 15176−15177. (n) Kuroki, M.; Asefa, T.; Whitnal, W.; Kruk, M.; Yoshina-Ishii, C.; Jaroniec, M.; Ozin, G. A. *J. Am. Chem. Soc.* **2002**, *124*, 13886−13895. (o) Tian, Z. R.; Liu, J.; Voigt, J. A.; Mckenzie, B.; Xu, H. *Angew. Chem., Int. Ed.* **2003**, *42*, 414−417. (p) Muth, O.; Schellbach, C.; Froba, M. *Chem. Commun.* **2001**, 2032−2033. (q) Matos, J. R.; Kruk, M.; Mercuri, L. P.; Jaroniec, M.; Asefa, T.; Coombs, N.; Ozin, G. A.; Kamiyama, T.; Terasaki, O. *Chem. Mater.* **2002**, *14*, 1903−1905. (r) Zhang, L.; Zhang, W.; Shi, J.; Hua, Z.; Li, Y.; Yan, J. *Chem. Commun.* **2003**, 210−211.

(7) (a) Asefa, T.; Ozin, G. A.; Grondey, H.; Kruk, M.; Jaroniec, M. *Stud. Surf. Sci. Catal.* **2002**, *141*, 1−26. (b) Alvaro, M.; Ferrer, B.; Fornes, V.; Garcia, H. *Chem. Commun.* **2001**, 2546−2547. (c) Alvaro, M.; Ferrer, B.; Garcia, H.; Rey, F. *Chem. Commun.* **2002**, 2012−2013. (d) Hossain, K. Z.; Mercier, L. *Adv. Mater.* **2002**, *14*, 1053.

(8) Shea, K. J.; Loy, D. A. *Chem. Mater.* **2001**, *13*, 3306−3319.

(9) (a) Macquarrie, D. J.; Jackson, D. B.; Mdoe, J. E. G.; Clark, J. H. *New J. Chem.* **1999**, *23*, 539−544. (b) Jaenicke, S.; Chuah, G. K.; Lin, X. H.; Hu, X. C. *Microporous Mesoporous Mater.* **2000**, *35−36*, 143−153. (c) Zheng, S.; Gao, L.; Guo, J. *J. Solid State Chem.* **2000**, *152*, 447−452.

(10) (a) Diaz, J. F.; Balkus, K. J.; Bedioui, F.; Kurshev, V.; Kevan, L. *Chem. Mater.* **1997**, *9*, 61−67. (b) Yoshitake, H.; Yokoi, T.; Tatsumi, T. *Chem. Mater.* **2002**, *14*, 4603−4610.

(11) (a) Dubois, G.; Corriu, R. J. P.; Reyé, C.; Brandès, S.; Denat, F.; Guilard, R. *Chem. Comm.* **1999**, 2283−2284. (b) Sutra, P.; Brunel, D. *Chem. Comm.* **1996**, 2485−2486.

(12) Silicycle Chemical Company (www.silicycle.com) sells many organic-functionalized and organoamine-functionalized silica gels for commercial uses as insoluble supports for solid-phase synthesis, as scavengers, catalysts or reagents.

(13) Evans, J.; Zaki, A. B.; El-Sheikh, M. Y.; El-Safty, S. A. *J. Phys. Chem. B* **2000**, *104*, 10 271−10 281.

(14) (a) Ito, T.; Nozaki, T.; Ishikawa, H. *J. Electrochem. Soc.* **1980**, *127*, 2053−2057. (b) Brinker, C. J. *J. Am. Ceram. Soc.* **1982**, *65*, C4−C5. (c) Inoue, H.; Komeya, K.; Tsuge, A. *J. Am. Ceram. Soc.* **1982**, *65*, C-205. (d) Brinker, C. J.; Haaland, D. M. *J. Am. Ceram. Soc.* **1983**, *66*, 758−765 (e) Kamiya, K.; Ohya, M.; Yoko, T. *J. Non-Cryst. Solids* **1986**, *83*, 208−222. (f) Lednor, P. W.; de Ruiter, R. *J. Chem. Soc., Chem. Commun.* **1989**, 320−321. (g) Brow, R. K.; Pantano, C. G. *J. Am. Ceram. Soc.* **1987**, *70*, 9−14. (h) Hayafuji, Y.; Kajiwara, K. *J. Electrochem. Soc.* **1982**, *129*, 2102−2108. (i) Ito, T.; Nakamura, T.; Ishikawa, H. *J. Electrochem. Soc.* **1982**, *129*, 184−188. (j) Zhang, S.-C.; Cannon, W. R. *J. Am. Ceram. Soc.* **1984**, *67*, 691−695. (k) Sekine, M.; Katayama, S.; Mitomo, M. *J. Non-Cryst. Solids* **1991**, *134*, 199−207. (l) Unuma, H.; Yamamoto, M.; Suzuki, Y.; Sakka, S. *J. Non-Cryst. Solids* **1991**, *128*, 223−230. (m) Baumvol, I. J. R.; Stedile, F. C.; Ganem, J.-J.; Trimaille, I.; Rigo, S. *J. Electrochem. Soc.* **1996**, *143*, 1426−1434.

(15) (a) El Haskouri, J.; Cabrera, S.; Sapiña, F.; LaTorre, J.; Guillem, C.; Beltrán-Porter, A.; Beltrán-Porter, D.; Marcos, M. D.; Amorós, P. *Adv. Mater.* **2001**, *13*, 192−195. (b) Inaki, Y.; Kajita, Y.; Yoshida, H.; Ito, K.; Hattori, T. *Chem. Comm.* **2001**, 2358−2359. (c) Wan, K.; Liu, Q.; Zhang, C. *Chem. Lett.* **2003**, *32*, 362−363.

(16) Rovai, R.; Lehmann, C.; Bradley, J. S. *Angew. Chem., Int. Ed.* **1999**, *38*, 2036−2038.

(17) (a) Kaskel, S.; Farrusseng, D.; Schlichte, K. *Chem. Commun.* **2000**, 2481−2482. (b) Kaskel, S.; Schlichte, K. *J. Catal.* **2001**, *201*, 270−274. (c) Farrusseng, D.; Schlichte, K.; Spliethoff, B.; Wingen, A.; Kaskel, S.; Bradley, J. S.; Schuth, F. *Angew. Chem., Int. Ed.* **2001**, *40*, 4204−4207.

Scheme 1. Ammonolysis Experimental Set-up

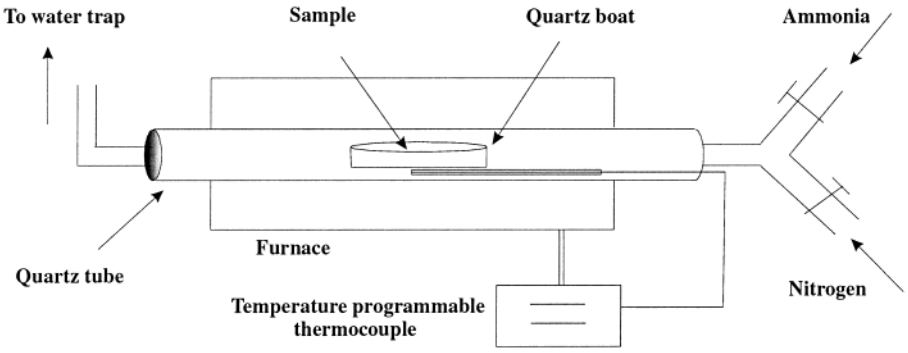

Here, we report a route to periodic mesoporous aminosilicas (PMAs) via ammonolysis of PMOs. For this, cubic and 2-D hexagonally ordered methylenesilicas and hexagonally ordered ethylensilica were subjected to ammonolysis. The substitution of organic and siloxane linkages in the PMOs by amine and nitride groups was achieved by treating the samples under ammonia gas at elevated temperatures. Concomitantly, thermal transformations of bridging methylene to terminal methyl groups or the loss of the organic groups took place. The PMAs produced from PMOs were compared with those obtained from periodic mesoporous silicas (MCM-41) under similar ammonolysis conditions. The ammonolysis of ordered mesoporous silicas has been reported earlier by others.[15] In particular, Marcos et al.[15a] reported that ammonolysis of MCM-41 produces ordered mesoporous silicon oxynitrides. Inaki et al.[15b] carried out ammonolysis of FSM-16 silica (which is structurally similar to MCM-41) and used the resulting material as catalyst in the Knoevenagel condensation. Most recently, Wan et al.[15c] reported results of ammonolysis of SBA-15 silica. We show herein that the ammonolysis of PMOs yields materials with improved stability relative to PMAs obtained from ammonolysis of MCM-41. The ammonolysis of PMOs described herein appears to be a much more successful nitridation method in terms of the achievable nitrogen loading than the reaction with nitrogen, which allowed others[18] to introduce low loadings of nitrogen (well below 1 wt %) into the silica framework. The ammonolysis of PMOs offers an additional opportunity for the synthesis of nitrogen-containing organosilicas with framework or pendent organic groups. PMAs with framework Si−N linkages represent a new class of materials that have already shown solid base catalytic activity in Knoevenagel reactions[15b] and bode well for a range of novel applications in the future.

Experimental Section

Materials. Tetraethyl orthosilicate (TEOS) (99.99%) and cetyltrimethylammonium bromide (CTABr) were purchased from Aldrich. NH_3 solution (NH_4OH, 37%) and HCl (36%) were obtained from BDH. Methanol was supplied by ACP. Bis-(triethoxysilyl)methane (BTM) and bis(triethoxysilyl)ethylene (BTE) were obtained from Gelest and were used as supplied. Anhydrous ammonia was purchased from Matheson while $^{15}NH_3$ was obtained from Cambridge Isotope Laboratories.

Preparation of PMAs. 2-D hexagonal mesoporous methylene-silica,[6e] ethylenesilica,[6a] and MCM-41[1a,b,6a] materials were synthesized by previously reported procedures through the hydrolysis and condensation of bis(triethoxysilyl)organic or TEOS precursors in the presence of surfactant under basic conditions. Unless otherwise noted, 100% precursor was used in each case to prepare the materials. Methylenesilica PMO with cubic structure[19] was synthesized as follows: A molar ratio of 1.00 Si: 0.24 CTABr: 134.07 H_2O: 6.44 NH_4OH was used for a typical synthesis. A solution of CTABr (1.34 g, 3.68 mmol), ammonium hydroxide (10.18 g, 35.05 wt %, 0.10 mol) and water (30.73 g, 1.71 mol) was stirred at room temperature for 30 min. To this solution was added BTM (2.63 g, 7.72 mmol), and the mixture was further stirred for 30 min, during which time a white precipitate formed. The material was then aged in its supernatant at 80 °C for 4 d and the product was filtered, washed with copious amounts of water, and dried under ambient conditions. A fine white powder was obtained (1.5 g).

Surfactant was removed from all the materials through acid/methanol washing.[6a] In some cases, the same surfactant-extracted material was divided into two parts and one fraction was dried under vacuum at 150 °C for >12 h (denoted with prefix "Dried"), whereas the other fraction was used directly after drying under ambient conditions (denoted with prefix "Undried"). These materials were then kept in a temperature programmable furnace and flushed with N_2 for 10 min and then with NH_3 at a rate of 7−10 mL/min for 10 min (the experimental setup is shown in Scheme 1). Next, the temperature was raised to 400 °C within 30 min and maintained at this temperature for 30 min under a flow of NH_3 to remove any residual surfactant. The temperature was kept either at 400 °C for another 4 h, or further raised over a period of 20 min to 550, 600, 700, and 850 °C, and maintained there for 4 or 8 h. Various series of materials were prepared following the same procedure from undried or dried, well-ordered or less-ordered cubic methylene-silicas; dried and undried 2-D hexagonal methylenesilicas; undried ethylenesilica; and dried and undried MCM-41 (see Table 1). After ammonolysis was complete, the samples were left inside the furnace to cool to room temperature (RT) under NH_3, after which they were flushed with N_2 for 20 min.

To enrich the samples with ^{15}N for the purpose of ^{15}N NMR spectroscopic measurements, the setup shown in Scheme 2 was connected to a furnace using a needle valve. Dried samples were kept inside the furnace and both the sample and the setup were outgassed under vacuum at RT. Then all of the $^{15}NH_3$ gas in A was condensed into B using liquid N_2 cooling by opening valves 1 and 2, and closing valve 3. Then, valve 1 was closed and a known amount (ca. 20 mmol) of NH_3 from the

(18) Kapoor, M. P.; Inagaki, S. *Chem. Lett.* **2003**, 94−95.

(19) Asefa, T.; Kruk, M.; Coombs, N.; Petrov, S.; Jaroniec, M.; Ozin, G. A., unpublished results.

Scheme 2. Ammonolysis Experimental Set-up for Handling ^{15}N Enriched Ammonia Gas

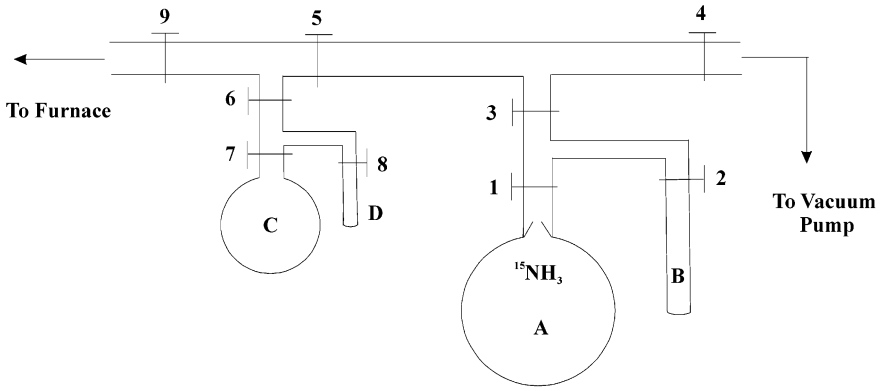

Table 1. Unit-cell Dimensions, a_o, and wt % Nitrogen and Carbon for PMOs and MCM-41 Materials before and after Ammonolysis

samples[a]	a_o (Å)[b]	wt % N	wt % C
cubic, well-ordered, undried methylene PMO			
Surfactant-extracted	130.4		
400 °C, 4 h	123.2	0.05	
550 °C, 4 h	125.7	2.61	
700 °C, 4 h	110.7	7.37	1.63
850 °C, 4 h	106.4	19.48	1.07
cubic, less-ordered, undried methylene PMO			
400 °C, 4 h	133.5	0.11	9.46
550 °C, 4 h	130.6	0.2	7.57
700 °C, 4 h	113.4	1.46	0.77
850 °C, 4 h	118.3	5.49	0.13
cubic, less-ordered, dried methylene PMO			
400 °C, 4 h	126.6	0.18	
550 °C, 4 h	123.9	0.34	
700 °C, 4 h	115.4	4.61	
850 °C, 4 h	110.2	7.89	
hexagonally ordered, undried, methylene PMO			
surfactant-extracted	50.2		
400 °C, 4 h	49.5	0.25	9.46
550 °C, 4 h	49.0	1.01	7.95
700 °C, 4 h	44.9	1.58	0.87
850 °C, 4 h	42.2	9.17	0.09
hexagonally ordered undried, ethylene PMO			
surfactant-extracted	48.3		
400 °C, 4 h	47.2	0.2	13.92
550 °C, 4 h	43.9	1.01	8.7
700 °C, 4 h	39.8	2.24	3.24
850 °C, 4 h	34.2[c]	5.73	0.23
hexagonally ordered, undried MCM-41			
surfactant-extracted	48.2	0.01	
400 °C, 4 h	45.5	1.14	
550 °C, 4 h	45.5	0.95	
700 °C, 4 h	45.3	3.95	
850 °C, 4 h	44.7	9.10	
hexagonally ordered, dried MCM-41			
surfactant-extracted	48.3	0.05	
400 °C, 4 h	46.3	0.76	
550 °C, 4 h	46.0	0.57	
700 °C, 4 h	43.0	2.68	
850 °C, 4 h	41.9	5.45	

[a] The degree of order of the materials was qualitatively determined on the basis of the PXRD patterns. The cubic samples with various degree of order were obtained for slightly different surfactant contents in the synthesis mixture. [b] $a_o = 2d_{100}/\sqrt{3}$ (Å) for 2-D hexagonally ordered materials, and $a_o = d_{hkl}\sqrt{N}$ (Å), $N = \sqrt{(h^2 + k^2 + l^2)^{1/2}}$ for cubic materials, major peak was considered as (210) reflection ($h = 2$, $k = 1$, $l = 0$) of $Pm3n$ or $Pm3m$ structure. [c] Very weak XRD peak.

condensate was transferred and condensed into D. Valve 5 was closed and the gas in C and D was permitted to flow into the furnace. Two samples were prepared in this way at 550 and 850 °C (samples were kept at these temperatures for 4 h). After ammonolysis, the samples were cooled inside the furnace, then flushed with N_2 for 20 min.

Instrumentation. Powder X-ray diffraction (PXRD) patterns were measured with a Siemens D5000 diffractometer using Ni-filtered Cu−K_α radiation with $\lambda = 1.54178$ Å. TEM images were recorded on a Philips 430 microscope operating at an accelerating voltage of 100 kV. Nitrogen adsorption measurements were carried out at 77 K on a Micromeritics ASAP 2010 volumetric adsorption analyzer. Before the measurements, the samples were outgassed under vacuum at 100 or 140 °C. Solid-state NMR spectra, ^{13}C cross-polarization magic angle spinning (CP-MAS) and ^{13}C nonquaternary suppression (NQS) CP-MAS (100.6 MHz), ^{29}Si CP-MAS (79.5 MHz) and ^{15}N MAS NMR (40.5 MHz) spectra were all obtained with a Bruker DSX400 spectrometer. Experimental conditions: ^{13}C CP-MAS NMR, 6.5 kHz spin rate, 2.5 ms contact time, 3 s recycle delay, 20 000 scans; ^{13}C NQS CP-MAS NMR experiment, 6.5 kHz spin rate, 3 s recycle delay, 50 μs dephasing time, 2000 scans; ^{29}Si MAS NMR, 6.5 kHz spin rate, 100 s recycle delay, 800 scans; ^{29}Si CP-MAS NMR, 6.5 kHz spin rate, 5 s recycle delay, 10 ms contact time, $\pi/2$ pulse width of 6.0−7.5 μs, 5000−8000 scans; ^{15}N CP-MAS NMR, 6.5 kHz spin rate, 5 s recycle delay, 2 ms contact time, $\pi/2$ pulse width of 13 μs, 2000 scans; and ^{15}N MAS NMR, 6.5 kHz spin rate, 5 s recycle delay, 2000 scans were used. Adamantane (major peak, 38.4 ppm vs. TMS), Si-$[Si(CH_3)_3]_4$ (major peak, −9.98 ppm vs. TMS) and ^{15}N-enriched glycine (−10 ppm) were used as external references for ^{13}C and ^1H, ^{29}Si, and ^{15}N NMR spectra, respectively.

Results and Discussion

Ammonolysis of PMOs and MCM-41. The powder X-ray diffraction patterns for well-ordered undried cubic methylenesilica, undried 2-D hexagonal methylenesilica, undried 2-D hexagonal ethylenesilica PMOs, and undried and dried MCM-41 materials before and after ammonolysis are shown in Figure 1. The ordered mesostructures of both the hexagonal and cubic methylene PMOs were retained after ammonolysis up to 850 °C. However, there was a decrease in *d* spacing corresponding to the major low angle reflection, the extent of which was found to be dependent on the starting material used, ammonolysis time, and temperature. A significant structural collapse was observed only for the PMA obtained from ethylenesilica PMO after ammonolysis at 850 °C for 4 h (Figure 1C). The decrease in the value of the *d* spacing for the hexagonal mesoporous materials after ammonolysis was observed to be in the order ethylenesilica PMO > methylenesilica PMO > MCM-41 (Δa_o = 14.1, 8.0, and 3.5 Å, respectively after ammonolysis at 850

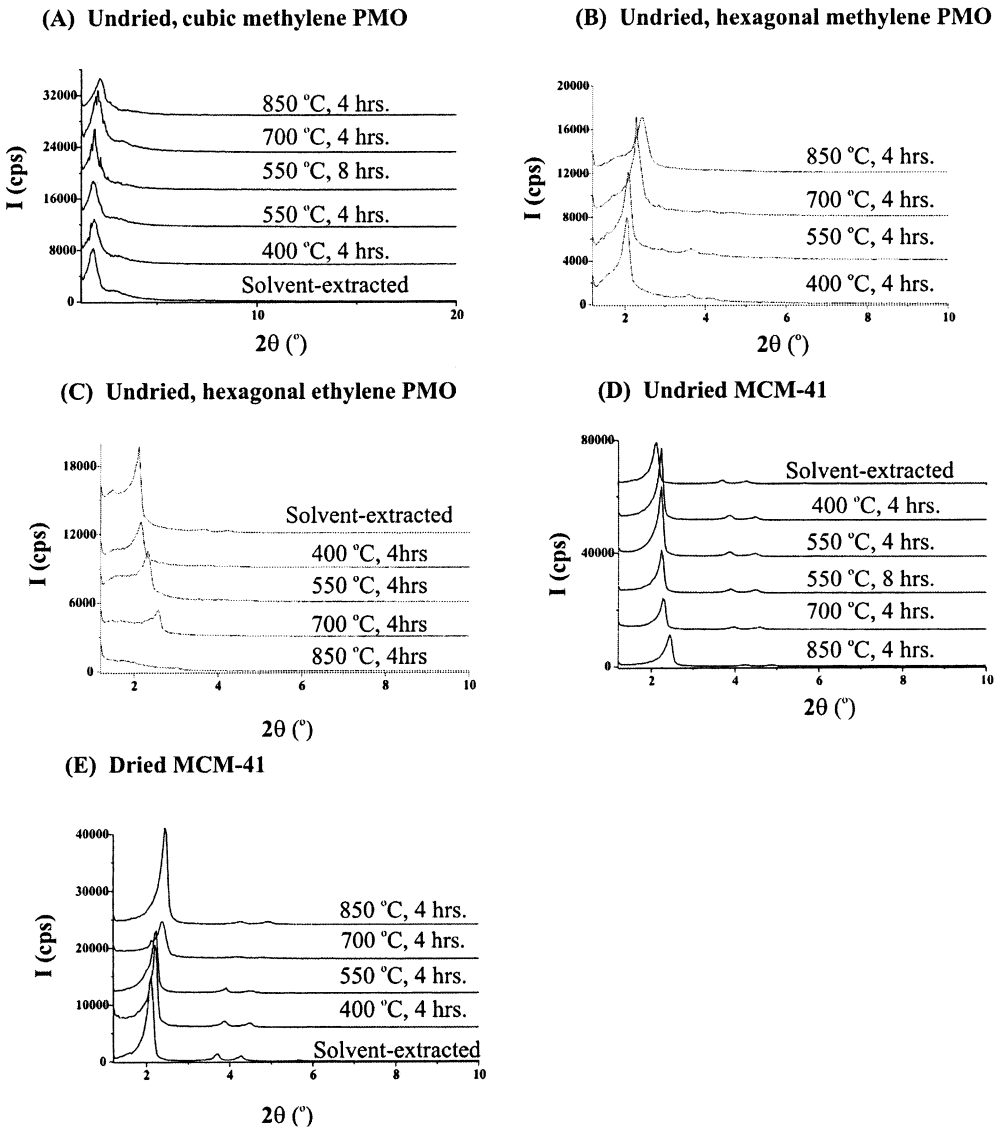

Figure 1. Powder X-ray diffraction (PXRD) patterns for (A) well-ordered, undried cubic methylene PMOs, (B) well-ordered, undried hexagonal methylene PMO, (C) well-ordered, undried hexagonal ethylene PMO, (D) well-ordered, undried hexagonal MCM-41, (E) well-ordered, dried hexagonal MCM-41 before and after ammonolysis at 400 °C, 550 °C, 700 °C, and 850 °C for 4 and/or 8 h.

°C for 4 h, $a_o = 2d_{100}/\sqrt{3}$). This observation can be explained when one considers that Si−X−Si linkages of different size (X = O, CH_2 or C_2H_2) are substituted by Si−NH−Si linkages in addition to an intrinsic silanol-condensation-induced shrinkage in all materials. The replacement of Si−CH_2−Si and Si−CH_2-CH_2−Si linkages in PMOs by Si−O−Si or Si−NH−Si linkages is expected to account for part of the reduction in size of the unit cell although the effect in methylenesilica PMO is anticipated to be small as the differences in Si−X−Si bond lengths among Si−CH_2−Si, Si−O−Si, and Si−NH−Si are not large (ca. 1.85, 1.50 and 1.57 Å for Si−C(sp^3), Si−O and Si−N(sp^3) bond lengths, respectively).[20]

Transmission electron microscopy (TEM) images of PMA samples revealed the presence of a cubic or hexagonal ordered structure before and after ammonolysis. A TEM image of a PMA sample obtained through the ammonolysis of undried cubic methylene PMOs is shown in Figure 2. A projection showing a square lattice can be seen. The structural analysis of cubic methylene PMOs synthesized under similar conditions indicated that these materials exhibit a *Pm*3*n* or *Pm*3*m* space group. The unit cell dimensions of the cubic PMAs formed from ammonolysis of the parent PMOs are listed in Table 1.

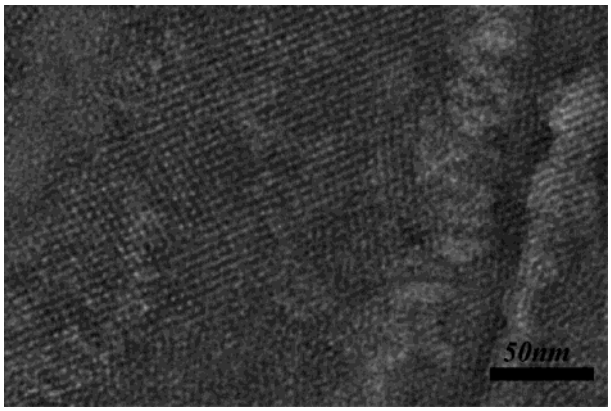

Figure 2. TEM image of well-ordered mesoporous cubic aminosilica after ammonolysis at 550 °C for 4 h.

The substitution of siloxane (−O−) and organic linkages (−R−) by amine groups during ammonolysis and the quantity

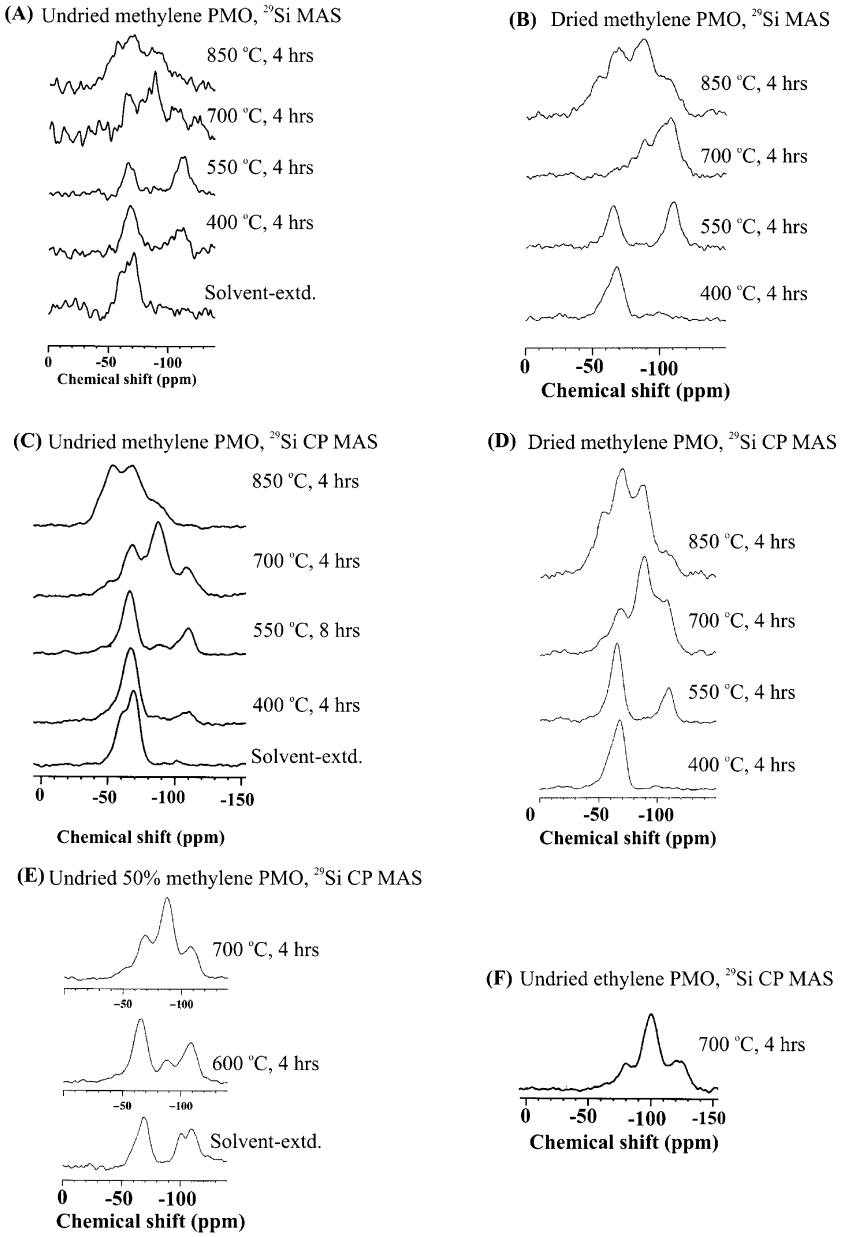

Figure 3. ^{29}Si CP-MAS and ^{29}Si MAS NMR spectra of dried and undried cubic methylene and hexagonal ethylene PMOs after ammonolysis at temperatures shown in the graph.

of amine groups incorporated into PMOs and MCM-41 silicas were monitored by ^{13}C CP-MAS, ^{29}Si CP-MAS, and ^{29}Si MAS, ^{15}N CP-MAS NMR spectroscopies, X-ray photoelectron spectroscopy, elemental analysis, and gas adsorption. The ^{29}Si NMR experiments were particularly useful for probing the relative number and nature of amine groups bonded to silicon atoms, because the replacement of oxygen and organic groups around silicon atoms in the PMO structures results in a downfield shift of ^{29}Si NMR peaks from ca. −110 for *Si* $(-O-)_4$ (Q^4 sites), −87 ppm for $(-O-)_3Si-NH_2-Si$ and −67 ppm for $(-O-)_3Si-CH_2-Si$ (T sites) to −46 ppm for $Si(-N=)_4$. When one takes into account the number of particular atoms bonded to each silicon atom, these trends are at least qualitatively consistent with the order of electronegativity of C, N, and O. The ^{29}Si CP-MAS and ^{29}Si MAS NMR spectra (Figure 3) after ammonolysis of methylene PMO up to 550 °C for 4 h showed the appearance and increase of peaks at −100 and −110 ppm corresponding to the formation of Q^3 and Q^4 sites, respectively, at the expense of the major T site centered at −67 ppm corresponding to $Si-CH_2-Si$ silicon atoms.[21] The new Q sites and the reduction of T peaks resulted from the replacement of $Si-CH_2-Si$ by $Si-O-Si$ and $Si-CH_3$ through nucleophilic attack by silanol Si−OH groups (for every such process the T peaks decrease roughly by the same amount as the Q peaks increase). The spectra also reveal a gradual appearance and

(20) (a) *CRC Handbook of Physics and Chemistry*, 83rd ed.; 2002−2003. (b) It should be noted here that for the sake of simplicity, some of the bonds formed by silicon atoms are not indicated in our notation of species in the silica, organosilica and organoaminosilica frameworks. For instance, $Si-CH_2-Si$ denotes a fragment in which methylene group is connected to two silicon atoms, and the three additional bonds on the each of the two silicon atoms are not explicitly noted and identified. It is assumed that in general, if *n* bonds are explicitly denoted for a given silicon atom, the remaining 4-*n* bonds are implied to be oxygen linkages with adjacent silicon atoms.

(21) It should be noted that Q^n sites are silicon atoms that are connected to *n* silicon atoms via oxygen bridges and to 4-*n* silanols (−OH groups), whereas T^n sites are silicon atoms that are connected to one carbon atom, to n silicon atoms via oxygen bridges, and to 3-*n* silanols.

increase of a new peak centered at −87 ppm at the expense of both the Q and T sites when the ammonolysis proceeds above 550 °C, possibly due to the replacement of Si−CH_2−Si by *Si*−NH_2 (and Si−CH_3) and even *Si*−NH−Si at later stages. However, the assessment of the nitrogen-containing groups is hard to make from the spectra due to the overlap of peaks corresponding to some of the *Si*−CH_2−Si and *Si*−NH−Si sites. Further analysis by quantitative ^{29}Si NMR spectra of samples that underwent ammonolysis at 550 °C for 8 h indicated that roughly half of the *Si*−CH_2−*Si* groups were converted to *Si*−O and *Si*−CH_3, whereas the amount of *Si*−NH_x sites was still small. However, the amount of incorporated nitrogen increased significantly when the samples were ammonolysed at 700 and 850 °C for 4 h. Moreover, when a 50% methylene-silica PMO (made from co-condensation of 50% BTM and 50% TEOS) was ammonolysed at 600 °C for 4 h, a new peak at −78 ppm corresponding to nitrogen-containing groups appeared at the expense of both Q and T sites, but it is still not clear whether this transformation proceeded through an initial conversion of Si−CH_2−Si to Si−O−Si, and later to Si−NH_x, or direct conversion of Si−CH_2−Si and Si−O to Si−NH_2. The spectra, however, clearly show the reduction of the Q sites at a higher rate than the reduction of T sites ($SiCH_2Si$) during ammonolysis of a 50% PMO. Various possible reactions that could take place during ammonolysis of PMOs and silicas (for instance, MCM-41, see below) are given in Schemes 3, 4, 5, and 6. Some of these reactions were already proposed to take place upon ammonolysis of silicas.[14d,14m]

We also performed ammonolysis experiments on MCM-41 materials under similar conditions as a control system to better determine the mode of conversion of PMOs to PMAs. The NMR results for ammonolysis of MCM-41 materials also showed downfield peaks (between −50 and −90 ppm) consistent with the formation of Si−N bonds (Supplementary Figure 1). These results were further corroborated by elemental analysis and XPS results (see below). Downfield peaks became more apparent when the ammonolysis was carried out at higher temperature and for a longer period of time indicating an increase in the substitution of oxides by amines. However, for the same ammonolysis times, the downfield peaks are less pronounced for MCM-41 than for PMOs, indicating a lower extent of conversion of MCM-41 to PMA. The major peak observed at −87 ppm in both PMO and MCM-41 materials after ammonolysis is attributed to Si atoms attached to a single nitrogen atom (*Si*−NH−Si or *Si*−NH_2).[15a] These results indicate that most of the ammonolysis reactions occur above 550 °C. The higher rate of conversion in PMOs is probably due to the transformation of Si−CH_2−Si into Si−NH_2 and Si−CH_3 groups making it easier to subsequently replace weaker Si−C bonds (Si−CH_3 groups for instance) by Si−N bonds. Ammonolysis of ethylene PMO also proceeds to PMA materials. However, the reduced thermal robustness and the more demanding structural rearrangements that must take place in ethylene PMO apparently make the resulting materials structurally unstable (Figures 1 and 3).

The ^{13}C CP-MAS NMR spectra (Figure 4A) show a gradual decrease of a peak at 0 ppm corresponding to methylene carbons during ammonolysis. Moreover, the formation of methyl groups (Si−CH_3) at ca. −0.4 ppm was observed under ^{13}C NQS CP-MAS NMR experimental conditions only in PMA samples that

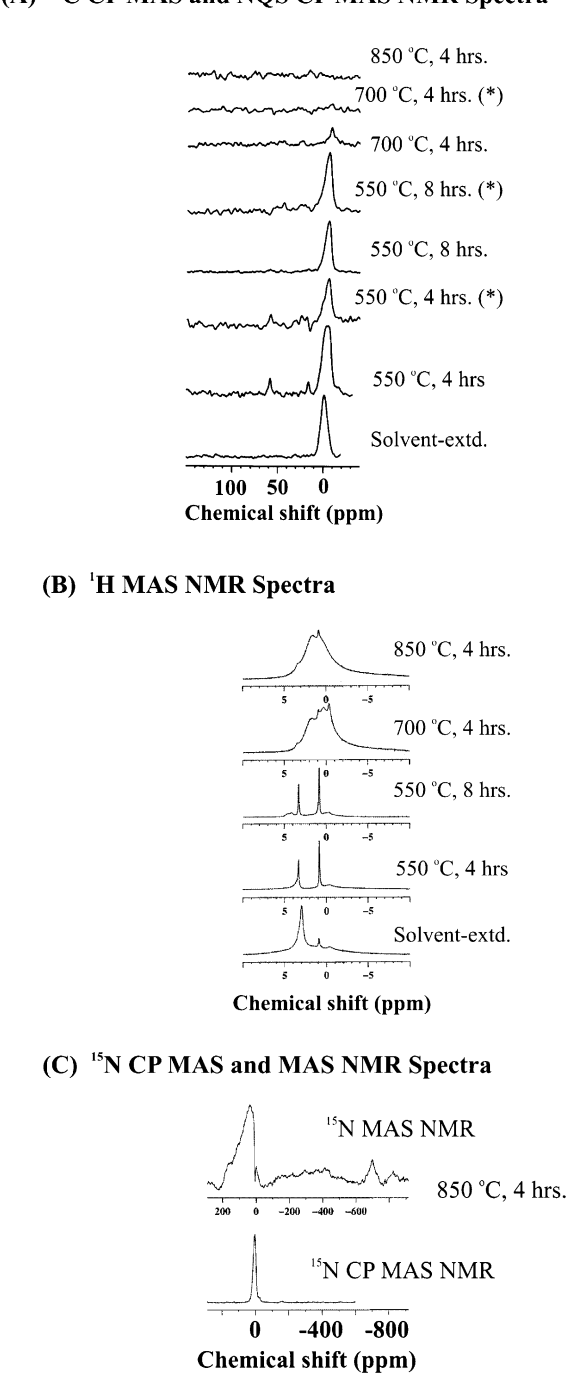

Figure 4. (A) ^{13}C CP-MAS and NQS CP-MAS NMR (indicated by asterisks), (B) ^{1}H MAS NMR, and (C) ^{15}N CP-MAS and MAS NMR spectra of PMOs after ammonolysis at temperatures shown in the graphs.

were thermolyzed under ammonia at 400 and 550 °C for 4 h. A very weak signal corresponding to methyl groups was also observed for samples treated at 700 °C for 4 h. The formation of methyl groups was likely due to the nucleophilic attack on Si atoms in Si−CH_2−Si either by Si−OH or NH_3 or Si−NH_2 groups resulting in Si−CH_3 and Si−O−Si linkages or Si−CH_3 and Si−NH_2 or Si−CH_3 and Si−NH−Si groups, respectively (Scheme 3). Similarly, nucleophilic attack may also occur via reaction with secondary amine (Si−NH−Si) groups formed during the ammonolysis. The absence of any organic moiety and the formation of higher content of tertiary amine, $(Si)_3N$

Scheme 3. Formation of *Primary* Amine Functionalized PMAs during Ammonolysis of PMOs and Silicas. (In the following schemes, the oxygen atoms are all shared by neighboring silicon atoms and so for example $O_{0.5}$ Represents Oxygen in Si−O−Si)

$$O_{1.5}Si\text{-}CH_2\text{-}SiO(OH) + NH_3 \longrightarrow O_{1.5}Si\text{-}CH_2\text{-}SiO(NH_2) + H_2O \quad (1)$$

$$O_{1.5}Si\text{-}O\text{-}SiO(OH) + NH_3 \longrightarrow O_{1.5}Si\text{-}O\text{-}SiO(NH_2) + H_2O \quad (2)$$

$$O_{1.5}Si\text{-}CH_2\text{-}SiO(OH) + NH_3 \longrightarrow O_{1.5}SiCH_3 + H_2NSiO(OH) \quad (3)$$

$$O_{1.5}Si\text{-}CH_2\text{-}SiO(OH) + NH_3 \longrightarrow O_{1.5}SiNH_2 + OSiCH_3(OH) \quad (4)$$

$$O_{1.5}Si\text{-}O\text{-}SiO(OH) + NH_3 \longrightarrow O_{1.5}SiOH + H_2NSiO(OH) \quad (5)$$

Scheme 4. Formation of *Secondary* Amine Functionalized PMAs during Ammonolysis of PMOs and Silicas

$$O_{1.5}SiNH_2 + O_{1.5}Si\text{-}CH_2\text{-}SiO_{1.5} \longrightarrow O_{1.5}Si\text{-}NH\text{-}SiO_{1.5} + O_{1.5}SiCH_3 \quad (6)$$

$$O_{1.5}SiNH_2 + O_{1.5}Si\text{-}O\text{-}SiO_{1.5} \longrightarrow O_{1.5}Si\text{-}NH\text{-}SiO_{1.5} + O_{1.5}SiOH \quad (7)$$

$$O_{1.5}SiNH_2 + O_{1.5}SiCH_3 \longrightarrow O_{1.5}SiNHSiO_{1.5} + CH_4 \quad (8)$$

$$O_{1.5}SiNH_2 + O_{1.5}SiOH \longrightarrow O_{1.5}SiNHSiO_{1.5} + H_2O \quad (9)$$

Scheme 5. Formation of *Tertiary* Amine Functionalized PMAs during Ammonolysis of PMOs and Silicas

$$O_{1.5}Si\text{-}NH\text{-}SiO_{1.5} + O_{1.5}Si\text{-}CH_2\text{-}SiO_{1.5} \longrightarrow (O_{1.5}Si)_3N + O_{1.5}SiCH_3 \quad (10)$$

$$O_{1.5}Si\text{-}NH\text{-}SiO_{1.5} + O_{1.5}SiCH_3 \longrightarrow (O_{1.5}Si)_3N + CH_4 \quad (11)$$

$$O_{1.5}Si\text{-}NH\text{-}SiO_{1.5} + O_{1.5}Si\text{-}O\text{-}SiO_{1.5} \longrightarrow (O_{1.5}Si)_3N + O_{1.5}SiOH \quad (12)$$

groups (a peak at ca. −48 ppm in ^{29}Si NMR spectra)[15a] were observed for PMOs and MCM-41 materials ammonolysed at 850 °C for 4 h (Scheme 5). The higher amount of $(Si)_3N$ could result in materials with unusual framework properties due to the substitution of more flexible Si−O−Si groups with rigid $(Si)_3N$ groups.[14]

Additionally, ^{1}H MAS NMR spectroscopy was used to further probe the substitution of organic and siloxane groups by primary, secondary and tertiary amine groups as ammonolysis temperature and time were increased. The spectrum for a solvent-extracted methylene PMO material shows two major peaks at ca. 0.9 and 2.9 ppm corresponding Si−C*H*$_2$−Si and Si−O*H* protons, respectively. After the materials were ammonolysed at 550 °C for 4 h, the intensity of the latter peak decreased due to dehydration and condensation processes. After 700 °C, however, a broad peak between 0 and 4 ppm appeared due to the formation of Si*N*H_x protons; the line broadening is likely caused by dipolar ^{1}H−^{14}N interactions.

For further investigations of amine functional groups in PMAs using ^{15}N NMR spectroscopy, samples were prepared via ammonolysis with ^{15}N-enriched ammonia. The ^{15}N CP-MAS NMR spectra (Figure 4C) show a peak at 7 ppm corresponding to Si−*N*H−Si or Si−*N*H$_2$ nitrogen atoms. Attempts to obtain quantitative ^{15}N MAS NMR spectra from the same material yielded only a very broad peak between 0 and 200 ppm due to the presence of various $(Si)_3N$ and Si*N*H_x sites in the material and some interference from nitrogen peaks arising from the presence of the BN stator in the probe.

Elemental analysis results (Figure 5 and Table 1) demonstrated that the wt. % of nitrogen introduced into the materials during ammonolysis depends highly on the temperature of the ammonolysis, and perhaps also on some other factors related to the starting materials. In most cases, the nitrogen contents we obtained for PMO and MCM-41 materials are comparable to those reported by El Haskouri et al.[15a] for mesoporous silicon oxynitrides prepared via ammonolysis at similar temperatures, despite the fact that the nitridation times were shorter in our case (4 h vs 12 h and more). One of the PMO materials we studied showed as high as ∼20 wt % nitrogen after ammonolysis for only 4 h, which is higher than the highest loading of nitrogen reported by El Haskouri et al. (15.5 wt % after ammonolysis of MCM-41 for 50 h). Wan et al. reported slightly higher nitrogen incorporation by ammonolysis of SBA-15 after longer times and higher temperatures.[15c] It should be noted that the definite comparison of the elemental analysis results for wt % N is difficult due to the possible presence of physisorbed ammonia in the samples, which were not treated under vacuum at high temperatures after the completion of the ammonolysis. Nonetheless, the weaker Si−C bond (in comparison to Si−O bond) is likely to have played some role by making the incorporation of nitrogen somewhat easier in the case of PMOs. However, it is clear that there is a continuous increase in the amount of nitrogen as the ammonolysis temperature was raised (Figure 5C).

X-ray photoelectron spectroscopy (XPS) results (Figure 6) show the presence of peaks at binding energies of ca. −104, −285, −400, and −533 eV corresponding to Si 2p, C 1s, N 1s, and O 1s ionization processes, respectively. Particularly noteworthy, the intensity of the N 1s peak increases concomitantly with the ammonolysis temperature and time indicating the incorporation of increasing amounts of nitrogen atoms into the materials at higher temperatures (Tables 2, 3).

The XPS results revealed interesting relationships in plots of binding energy vs ammonolysis temperature (Figure 7). The binding energy for N 1s decreases as more of the protons of ammonia or amine groups are substituted by more electropositive silicon atoms resulting in an overall trend of N 1s binding energy as NH_3 > Si−NH_2 > Si−NH−Si > $(Si)_3N$. Further, the binding energy for the silicon Si 2p core electrons decreases as more of the surrounding electronegative oxygen atoms are substituted by less electronegative nitrogen atoms. The decrease in Si 2p binding energy during ammonolysis strongly suggests a corresponding increase in the relative number of tertiary and secondary amine groups, that is, there is an increase in the number of nitrogen atoms around the silicon atoms. Similar binding energy curves have also been reported for microporous silica films that underwent ammonolysis.[14g] Unfortunately, due to the fact that XPS is a surface sensitive technique, quantitative N wt % data for the bulk sample are not attainable from XPS.

Overall, the above results indicate the likelihood of several possible reactions (Schemes 3−6) proceeding simultaneously in PMOs during ammonolysis. Some of these are also possible during ammonolysis of MCM-41 silicas,[15] silica gels, and glasses.[14] In cases of both PMO and MCM-41, the conversion of Si−OH and Si−O−Si groups to Si−NH_2 could occur through the reaction with ammonia. In addition, in methylene PMOs, an additional thermal transformation of bridging methylene into terminal methyl groups, for instance due to a nucleophilic attack by silanol or NH_3, could take place.Similar organic group transformations are known to occur in the same temperature range when the methylenesilica PMOs are pyrolyzed under air.[6e] It should be noted here that in the case of undried samples, the

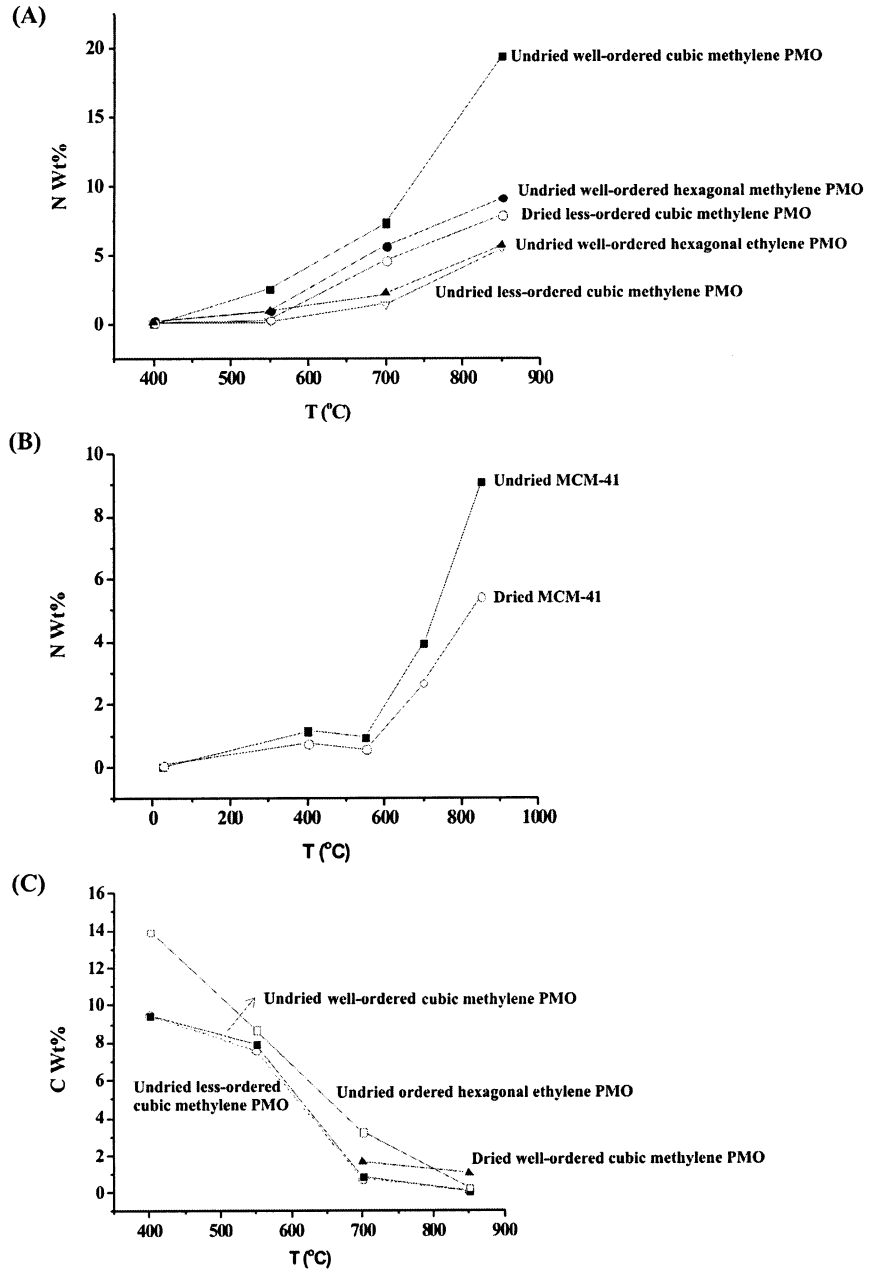

Figure 5. Elemental analysis results: Nitrogen wt. % for (A) ammonolysed PMOs and (B) ammonolysed MCM-41, and (C) carbon wt. % for ammonolysed PMOs.

content of silanols (Si−OH) is likely to be higher than in the case of the dried materials, which could facilitate reactions 1 and 3 (Scheme 3). Furthermore, the physisorbed water in the undried materials can react with ammonia to form ammonium hydroxide, which is a base that can catalyze hydrolysis processes, such as a transformation of siloxane bridges to silanols. The effect of the concentration of silanol groups on the formation of siliconoxycarbides is known.[22] Hence, water may indirectly facilitate the ammonolysis processes by increasing the silanol concentration through the base-catalyzed hydrolysis of some Si−O−Si and Si−CH_2−Si bonds (Scheme 6). It is expected that at lower temperatures, primary amines form in relatively larger quantity, and are subsequently converted to secondary and tertiary amine groups as the ammonolysis temperature and time increase (Schemes 4 and 5). Furthermore, the presence of the organosilica groups in the PMOs seems to facilitate the ammonolysis as the weaker Si−C bonds are likely to be more susceptible to substitution with nitrogen than the Si−O bonds. The facilitation of ammonolysis by the presence of Si−C bonds has been reported in the literature.[14e,l,23] For instance, 6 wt. % of nitrogen could be incorporated by ammonolysis into a silica with pendent methyl groups, whereas only a small amount of nitrogen was introduced in a silica gel under similar conditions.[14e] In another study, it was concluded that gels with organic bridging groups may be the best precursors for the synthesis of oxynitride silica glasses via ammonolysis.[23]

Nitrogen adsorption provided much additional insight into the ammonolysis process. Nitrogen adsorption isotherms measured at 77 K for well-ordered, cubic methylenesilica PMO subjected to the ammonolysis at different temperatures are

(22) Liu, Q.; Shi, W.; Babonneau, F.; Interrante, L. V. *Chem. Mater*. **1997**, *9*, 2434−2441.

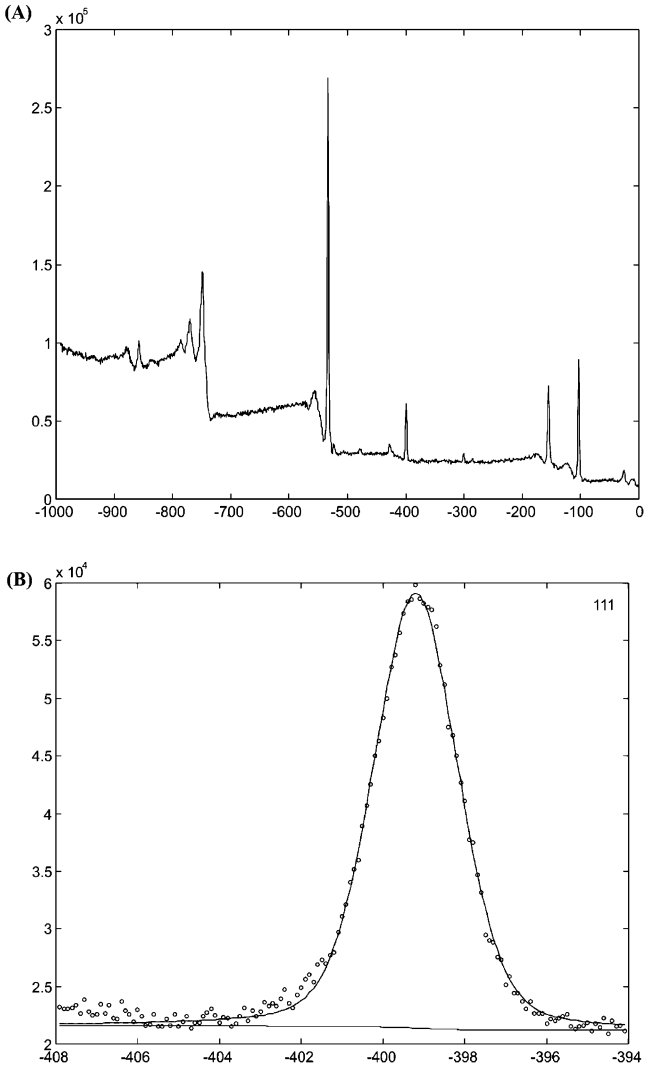

Figure 6. (A) X-ray photoelectron spectrum for well-ordered PMOs ammonolysed at 850 °C for 4 h. (B) Enlarged N 1s peak in the above spectrum after 4 h.

Table 2. Nitrogen and Silicon Binding Energies and Surface Atomic Composition for Undried Methylene PMO Samples after Ammonolysis (ref C1s 284.6 eV)

ammonolysis temperature (°C)	N 1s	N at. %[a]	Si 2p	Si at. %[a]
400	−397.9	0.24	−102.9	29.67
550	−400.8	0.40	−102.9	28.29
700	−398.4	4.43	−103.1	29.99
850	−397.8	2.43[b]	−102.7	29.90

[a] The atomic % composition for N and Si obtained here from XPS do not reflect the bulk composition of the sample (which is assessed using elemental analysis of ^{29}Si MAS NMR), because XPS provides information about the composition of the surface layer only. [b] The unexpected lowering in the N at. % for this particular sample compared to the sample pyrolyzed at 850 °C may be an indication that the XPS measurement does not give a clear and true picture of the bulk composition of the materials (see text below).

shown in Figure 8. It can be seen that the nitrogen gas uptake decreased as the ammonolysis temperature was increased. Concomitantly, the capillary condensation step (observed at relative pressures somewhere between 0.25 and 0.45, depending on the particular sample) shifted to lower pressures, which is

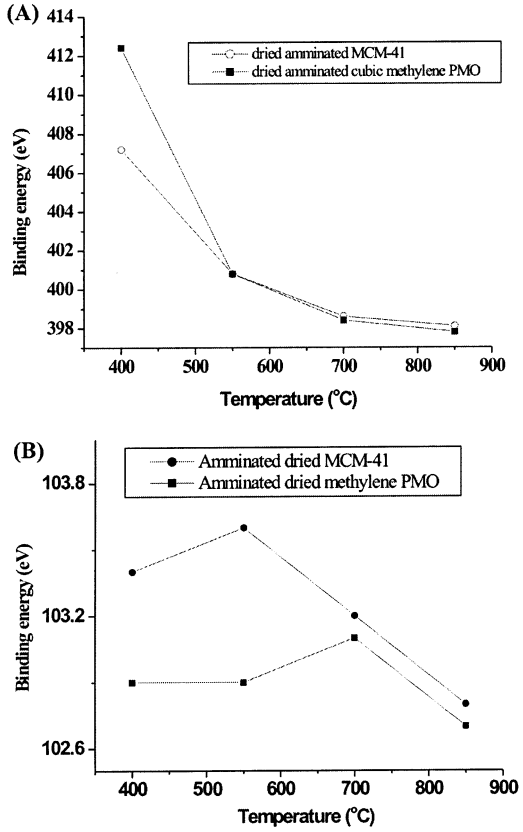

Figure 7. (A) N 1s and (B) Si 2p binding energy curves of ammonolysed PMO and MCM-41 materials.

Table 3. Nitrogen and Silicon Binding Energies and Surface Atomic Composition for Undried MCM-41 Samples after Ammonolysis (ref C1s 284.6 eV)

ammonolysis temperature (°C)	N 1s	at. %	Si 2p	at. %
400	−407.2	0.00	−103.4	29.26
550	−400.8	0.15	−103.6	29.57
700	−398.6	0.69	−103.2	30.01
850	−398.1	8.37	−102.8	22.17

Scheme 6. Possible Participation of Water Molecules and Hydroxide in Undried Samples Facilitating Ammonolysis Reactions

$$O_{1.5}Si\text{-}O\text{-}SiO_{1.5} + H_2O \xrightarrow{OH^-} 2\,O_{1.5}Si\text{-}OH \quad (13)$$

$$O_{1.5}Si\text{-}CH_2\text{-}SiO_{1.5} + H_2O \xrightarrow{OH^-} O_{1.5}Si\text{-}CH_3 + O_{1.5}Si\text{-}OH \quad (14)$$

$$O_{1.5}Si\text{-}CH_2\text{-}SiO_{1.5} + NH_3 \xrightarrow{OH^-} O_{1.5}Si\text{-}CH_3 + O_{1.5}Si\text{-}NH_2 \quad (15)$$

indicative of the pore size decrease. Interestingly, the capillary condensation step was clearly observed even for the sample ammonolyzed at 850 °C, which provides clear evidence for the preservation of ordered mesopores.[24] The pore size changes are clearly seen on the pore size distributions[24b] shown in Figure 9. The pore diameter decreased by up to ∼1 nm, when the PMO was ammonolyzed at temperatures up to 850 °C. This decrease was in a quite good agreement with the extent of the unit-cell size decrease observed using XRD. It is noteworthy that even after the ammonolysis at 850 °C, the resulting PMA (containing

(23) Belot, V.; Corriu, R.; Leclercq, D.; Mutin, P. H.; Vioux, A. *J. Non-Cryst. Solids* **1992**, *147*−*148*, 309−213.

(24) (a) Kruk, M.; Jaroniec, M.; Sayari, A. *Langmuir* **1997**, *13*, 6267−6273. (b) Kruk, M.; Jaroniec, M. *Chem. Mater.* **2001**, *13*, 3169−3183.

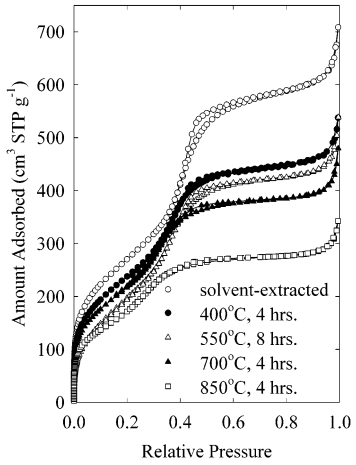

Figure 8. N_2 adsorption isotherms for well-ordered cubic methylene PMO before and after ammonolysis. The data for the sample treated at 400 °C were corrected to offset the distortion in the shape of the isotherm, which arose as a result of a very small weight of the sample used for the adsorption analysis.

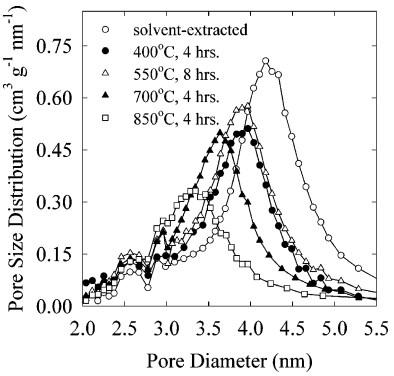

Figure 9. Pore size distributions for well-ordered cubic methylene PMO before and after ammonolysis.

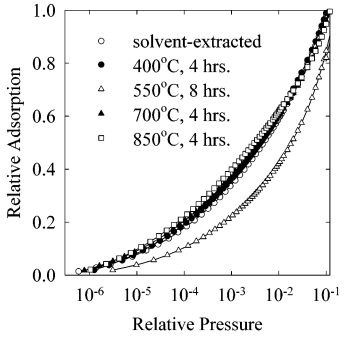

Figure 10. Low-pressure relative adsorption curves for well-ordered cubic methylene PMO before and after ammonolysis.

close to 20 wt % nitrogen) exhibited a specific surface area of ~600 m^2 g^{-1} and a total pore volume of ~0.5 cm^3 g^{-1}.

In addition, gas adsorption data provided valuable information about surface properties of PMAs. Shown in Figure 10 are relative adsorption curves[24b] for PMO sample subjected to ammonolysis at different temperatures. The relative adsorption is defined here as the amount adsorbed at a particular pressure divided by the monolayer capacity (estimated using the standard BET method). After the ammonolysis at 400 °C, the relative adsorption at low pressures slightly increased in comparison to that for the starting PMO. On the other hand, when the temperature was increased to 550 °C, a PMA material with a very low relative adsorption was obtained. Further increase in the ammonolysis temperature afforded PMAs with quite strong low-pressure relative adsorption, even stronger than that observed for the starting PMO. To understand these changes, one needs to know that the relative adsorption at low pressures reflects the strength of interactions between the surface of the material and the adsorbed gas (nitrogen in our case).[24b] It is well-documented that the introduction of hydrophobic organic groups on the silica surface may lead to a substantial reduction of the low-pressure relative adsorption of nitrogen, because of the weak interactions of nitrogen molecules with hydrophobic organic moieties.[24b] This weakening of low-pressure adsorption is typically more pronounced in the case of pendent organic groups on the silica surface than in the case of framework organic groups, most likely because of the lower degree of exposure of the latter to interactions with nitrogen molecules adsorbed on the surface. Indeed, the methylenesilica PMO exhibited a slight decrease in low-pressure adsorption when compared to the behavior of silicas. The ammonolysis at 400 °C did not bring about any major changes in the low-pressure adsorption because the framework organic groups are still retained after treatment at this temperature (as verified on the basis of elemental analysis results for methylenesilica PMO samples in the current study and earlier results[6e]). On the other hand, the treatment at 550 °C still did not result in any substantial loss of organic groups (as inferred from EA), but led to the transformation of the bridged organic groups (Si−CH_2−Si) to pendent groups (Si−CH_3), as demonstrated earlier in the case of heating of methylenesilica PMO under air as well as under ammonia. As discussed above, the presence of hydrophobic organic groups on the silica-based surface results in weaker interactions with nitrogen. Because of the high loading of the organic groups (one per two silicon atoms in the starting PMO), the resulting surface may exhibit very high coverage of methyl groups and thus be very hydrophobic and interact weakly with nitrogen. So, the significant reduction of the low-pressure adsorption observed after ammonolysis at 550 °C provides strong evidence for the presence of hydrophobic moieties on the material's surface, and these hydrophobic species may be identified as methyl groups on the basis of earlier studies. The fact that the samples subjected to ammonolysis at 700 and 850 °C exhibit low-pressure adsorption somewhat stronger than that for the starting PMO is consistent with a loss of most organic groups at these temperatures, as inferred from EA, which results in surface properties more similar to those of silicas. It appears that in contrast to the surface organic groups, the presence of various kinds of amine groups did not lead to any substantial differences in low-pressure nitrogen adsorption properties, when compared to silicas.

An earlier study of nitridation of silicas and organosilicas indicated that stability is a major issue in the synthesis of silicon oxynitrides, as some of them can lose much of their nitrogen content within months or even hours of exposure to ambient air.[25] This was paralleled by a rapid loss of the surface area from high to very low within weeks. In our case, MCM-41 samples subjected to ammonolysis underwent a structural collapse within weeks of storage, which manifested itself in a dramatic loss of the ordering as seen from XRD patterns. In

(25) Lednor, P. W.; de Ruiter, R. In *Inorganic and Metal-Containing Polymeric Materials*; Sheats, J. E., Carraher, C. E., Jr., Pittman, C. U., Jr., Zeldin, M., Currell, B., Eds.; Plenum Press: New York, 1990; p 187−195.

fact, the PMA samples derived from MCM-41 were so unstable that we were not able to acquire nitrogen adsorption isotherms that would be consistent with well-resolved XRD patterns measured days or weeks before. The adsorption capacity of these degraded PMAs was moderate (see Supporting Figure 2), the surface area was relatively low (on the order of 300 m^2 g^{-1} in some cases), and the pore diameter was often larger than the unit-cell size of the starting MCM-41 materials, which suggest a possibility of the loss of substantial parts of the pore walls. It was confirmed that the collapse progresses with time, leading to a gradual reduction of the specific surface area and pore volume for PMAs derived from MCM-41 silicas. These are the first reported results on the stability of PMAs obtained via ammonolysis of ordered mesoporous silicas, because earlier studies[15] did not provide information about the stability. On the basis of our work reported herein and earlier work of Lednor and de Ruiter,[25] one can expect that PMA samples obtained through the ammonolysis of ordered mesoporous silicas are likely to be unstable unless they are prepared at very high temperatures (close to 1100 °C).

The stability of PMAs derived from PMOs was found to be far superior to that of the aforementioned PMAs derived from MCM-41 silicas. Samples of well-ordered cubic methylenesilica PMO ammonolyzed at 400 and 550 °C did not undergo any degradation during storage over the period of many months, as seen from nitrogen adsorption data. The stability of these materials may be related to the presence of organic groups that increase the surface hydrophobicity that protects the surface from being attacked by water from the air, which is expected to be the cause of the collapse of PMAs during storage. As far as the PMA synthesized at 700 °C is concerned, its collapse became apparent after several months of storage, but even after that, the material retained much of its surface area and adsorption capacity. The collapse observed after several months for PMO-derived PMA synthesized at 850 °C was more severe, but still no evidence for the collapse was observed after the first several weeks of storage. These results indicate that PMOs are superior to MCM-41 as starting materials for the synthesis of stable PMAs via ammonolysis at temperatures studied (400−850 °C). One might suspect that the improved stability of PMAs derived from PMOs may arise from the possible presence of carbon deposits that may form under certain conditions when organic groups are treated at high temperature. However, in the case of our samples, the dark coloration characteristic of carbon deposit was not observed. Moreover, the samples subjected to ammonolysis at 700 and 850 °C had low carbon content, as determined by EA. So, the enhanced stability of PMAs derived from PMOs does not arise from the presence of any carbonaceous deposit. On the other hand, the presence of Si−C bonds in PMOs may facilitate the formation of PMAs with higher stability, because the Si−C bonds may be much easier to replace by nitrogen-containing species due to the relatively lower dissociation energy of the Si−C bond (ca. 90−100 kcal/mol) compared to Si−O (ca. 110 kcal/mol) The effect of the difference in bond dissociation energy between Si−C and Si−O bonds on the rate of thermal replacement reactions in similar polymeric carbosiloxane materials is known in the literature.[26] Further studies directed at improving the stability and increasing the loading of nitrogen in PMAs are highly desirable, and PMOs appear to be promising starting materials from this point of view.

Conclusions

A new synthetic route to periodic mesoporous aminosilicas, PMAs, via ammonolysis of periodic mesoporous organosilicas, PMOs, is reported. The incorporation of amine functional groups in the materials has been demonstrated by various characterization techniques. The largest wt. % nitrogen incorporated was found in undried cubic methylene PMO materials that underwent ammonolysis at 850 °C for 4 h. Because of the many possible nitrogen-containing framework and surface groups in PMA materials obtained by ammonolysis of PMOs, the concentration of which is dependent on the ammonolysis temperature and time, this approach provides an appealing pathway to a myriad of new mesoporous silica nanocomposites with multifunctional properties. Furthermore, we have demonstrated that the new pathway from PMOs resulted in more stable PMA materials compared to those resulting from MCM-41 materials. PMAs may find applications in base catalysis and gas separation, environmental remediation and controlled delivery of chemicals.

Acknowledgment. G.A.O. is a Canada Research Chair in Materials Chemistry. He acknowledges the financial support of the Natural Sciences and Engineering Research Council (NSERC) of Canada for this work. M.J. acknowledges support by NSF Grant CHE-0093707. T.A. acknowledges Dr. Srebri Petrov for valuable discussion regarding PXRD, respectively.

Supporting Information Available: Figure with ^{29}Si NMR data for MCM-41 samples before and after ammonolysis. Figure with nitrogen adsorption isotherms for MCM-41 silicas before and after ammonolysis (PDF). This material is available free of charge via the Internet at http://pubs.acs.org.

JA036080Z

(26) Bois, L.; Maquet, J.; Babonneau, F.; Mutin, H.; Bahloul, D. *Chem. Mater*. **1994**, *6*, 796−802.